Terra Antartica
1998, **5**(3), 367-374

Lonestone Abundance and Size Variations in CRP-1 Drillhole, Victoria Land Basin, Antarctica

J.D. BRINK[1], R.D. JARRARD[1], L.A. KRISSEK[2] & T.J. WILSON[2]

[1]Dept. of Geology and Geophysics, University of Utah, 135 S. 1460 E., Rm. 719, Salt Lake City UT 84112-0111 - USA
[2]Dept. of Geological Sciences, Ohio State University, 275 Mendenhall, 125 S. Oval Mall, Columbus, OH 43210 - USA

Received 17 July 1998; *accepted in revised form* 15 October 1998

Abstract - Lonestone abundances in CRP-1 were investigated using three methods: core examination at Cape Roberts Camp, analysis of digital core images and follow-up core examination. For all images of split-core, we determined size and depth of every detectable lonestone larger than 3 mm. Lonestone abundance decreases exponentially with clast size. Although no significant depth-dependent variations in lonestone size distribution were detected, a strong 0.5-0.7 m abundance periodicity, of unknown origin, is evident within diamicts. Lonestone volume percentage was estimated from size distribution; most size classes contribute approximately the same volume to the total. Sizes >16 mm have rare enough lonestones that their counts are nonrepresentative when based on short intervals of split core. This problem does not affect total counts significantly, but the volume analysis needs to be confined to ≤16 mm lonestones to avoid instability induced by rare and nonrepresentative larger lonestones.

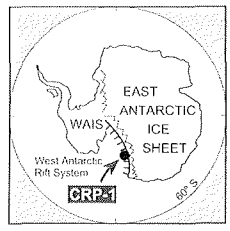

If lonestone abundance can be used as an indicator of glacial proximity, then our CRP-1 lonestone abundance logs confirm the overall character of previously inferred variations in relative distance to the ice margin. Large-scale changes in lonestone abundance also reflect the CRP-1 sequence stratigraphy, with individual sequences generally characterised by basal lonestone-rich diamict overlain by lonestone-poor sands and muds. The relationship between glacial proximity and lonestone abundance within diamicts and within sand-mud intervals is, however, less certain. For example, two or three gradual lonestone increases may indicate regressions during glacial advances, in contrast to the more common CRP-1 pattern of dominantly transgressive sequences.

INTRODUCTION

Lonestones are rock clasts of gravel or larger size, commonly derived from glacial processes, within a finer-grained sediment. Lonestone abundance may be an indicator of proximity of a site to its glacial source. Lonestone sphericity and roundness are often related to glacial sedimentary processes (Boulton, 1978; Domack et al., 1980; Sharp, 1982; Bennett et al., 1997), although a variety of other variables can obscure this relationship (Kirkbride, 1995). Lonestone fabric is more strongly developed in subglacially deposited sediments than in proglacial sediments (*e.g.* Hambrey, 1989).

Lonestones are nearly ubiquitous in cores from the first drillhole of the Cape Roberts Project, CRP-1. In the initial analysis of the CRP-1 cores, lonestone abundance variations were interpreted to be the primary indicator of glacial proximity (Cape Roberts Science Team, 1998). This paper determines lonestone abundance and size variations within CRP-1, in order to provide a foundation dataset for analyses of fluctuations in both glacial input and glacial proximity to CRP-1.

METHODS

We undertook three complementary analyses of lonestone abundances within CRP-1: core examination at Cape Roberts Camp (L_{CRC}), core image examinations at University of Utah (L_{UU}) and core examination at Florida State University (L_{FSU}). Multiple methods of lonestone analysis were necessary in order to evaluate the accuracy of lonestone abundance and size. Initial lonestone counts at Cape Roberts Camp did not include detailed records of clast size determinations. While lonestone analysis of core images did include number and size, certain ambiguities in the digital images had to be resolved with a second examination of the CRP-1 core at Florida State University.

As part of the initial core descriptions undertaken at Cape Roberts Camp, the number of lonestones (N_{CRC}) for each 10 cm interval throughout the CRP-1 cores was estimated by eye. Lonestones were distinguished from similar sized, non-lonestone clasts. The latter are mainly intraformational breccias and, more rarely, soft-sediment clasts. Other distinctive lonestone features, including size and lithology, were sometimes included in the core descriptions. The threshold size for counting was nominally 2 mm, the boundary between sand and gravel; however, the actual threshold size for N_{CRC} fluctuated downcore. Not every lonestone was counted when N_{CRC}>20 per 10-cm interval, so values >20 are subjective. These initial observations were presented graphically in the Initial Reports (Cape Roberts Science Team, 1998), with one modification: N_{CRC} values were clipped at a maximum of N_{CRC}≥5.

Prior to core description at Cape Roberts Camp, split cores were digitally photographed at the Cape Roberts

Drillsite. The methods are described, and reduced black-and-white images shown, in the CRP Initial Reports (Cape Roberts Science Team, 1998). The University of Utah lonestone identifications are based on computer analysis of the digital images. For all split-core images, we determined size, depth, and roundness of every detectable lonestone larger than 3 mm. Size was classified by overlaying the clast image with a template consisting of circles with the following sizes: 3, 4, 6, 8, 12, 16, 20, 24, 32, 40, 48, 56, and 64 mm (phi values of –1.6, -2, -2.6, -3, -3.6, -4, -4.3, -4.6, -5, -5.3, -5.6, -5.8, and –6, respectively). Roundness was subjectively estimated for the entire length of the split core according to the roundness scale of Pettijohn et al. (1987). On average the clasts were sub-rounded. However, there was no correlation of clast roundness with clast size or facies associations.

This lonestone image analysis initially included identification of 2-mm lonestones, in addition to the sizes above. However, these identifications were deemed to be highly subjective: 2-mm lonestones are represented by too few pixels for consistently accurate identification from the digital images, particularly when the color contrast between lonestone and matrix is subtle. Consequently, the counting threshold was increased to 3 mm, and no image-based 2-mm counts are included in this analysis.

Lonestone identifications from the split-core images (L_{UUs}) provide the primary dataset of this study, but whole-core images (obtained by rotating the whole core while scanning its outer surface) were similarly analysed (L_{UUw}). The advantage of the whole-core images is that the increment of available area per unit depth is increased by a factor of π over that from split cores. Accordingly, split-core lonestone abundance (N_{UUs}), the sum of lonestone identifications for all sizes (L_{UUs}), is tripled. The main disadvantage is that whole-core images were obtained for only about 18% of the cored interval, because only the most lithified whole cores could be imaged without risk of core damage. The outer core surface is commonly rougher than the corresponding portion of split-core surface, hampering identification of the smaller lonestones.

Editing of the UU lonestone counts included merging and reconciliation of image overlaps, identification of core gaps, and reconciliation of any depth differences between images and core descriptions. Only lonestones were tabulated; other gravel-sized clasts were excluded: intraformational clasts, soft sediment clasts, and fossils. Drilling-washed gravels, though consisting mainly of lonestones, were excluded because of both depth uncertainty and the sorting imposed by mud circulation.

Reliable lonestone identification on the split-core images was not always possible. The surface of some split cores was smeared, and a few images were slightly out of focus. Discrimination of lonestones from intraformational clasts and *in situ* brecciation was locally ambiguous based on core images alone. To resolve these ambiguities, cores were re-examined at Florida State University. In addition, lonestone counts were undertaken on selected 10-cm intervals, using a 10-cm template and a clast size template. For most intervals, the numbers of 3 mm and >3 mm lonestones were counted. For 39 intervals, the number of 2 mm lonestones was also counted, both for determination of the percentages of 2-mm lonestones relative to larger ones, and for detection of any variations in the size threshold employed in the N_{CRC} counts.

Based on the FSU core examinations, some editing of the N_{CRC} lonestone tabulations was undertaken. N_{CRC} intervals that were dominated by 2-mm lonestones were deleted, thereby calibrating the N_{CRC} data to a more uniform threshold of about 3 mm. This revised threshold is comparable to that used in the L_{UU} analyses, but the main reason for this editing was to reduce apparent downhole variations in lonestone abundance associated with threshold variations. Because the CRC counts were of total lonestones rather than of lonestone size distribution, it was necessary to delete intervals with 2-mm dominance rather than to edit their values. Zones dominated by intraformational clasts, flagged in the Initial Reports (Cape Roberts Science Team, 1998) or in FSU core examinations, were excluded from N_{CRC} data. Minor N_{CRC} deletions were undertaken in rare intervals for which lonestone identification was ambiguous because of broken core or mudstone clasts.

ANALYSIS

LONESTONE SIZE DISTRIBUTION

Lonestone size distribution was investigated primarily using the dataset based on the University of Utah split-core image analysis (L_{UUs}). Supporting data were provided by the whole-core images (L_{UUw}), but the confinement of whole-core images to mostly the lower part of CRP-1 restricts generalisations based on these data. Lonestone tabulations at Cape Roberts Camp (N_{CRC}) did not consider sizes. Most interval counts at Florida State University (L_{FSU}) distinguished only 3-mm and >3-mm lonestones, but for some intervals 2-mm lonestones were also counted. These 2-mm counts permit extrapolation of patterns to smaller sizes than those encompassed by the L_{UUs} results.

Based on the L_{UUs} dataset of 2 793 points, and the L_{UUw} dataset of 3 356 points, overall lonestone abundance decreases approximately exponentially with increasing clast size (Fig. 1). Each size class has about twice as many lonestones as the next larger size class, and about the same number as all larger sizes combined. For example, half of all identified lonestones are within the smallest size classification, 3 mm. A perfect exponential relationship (corresponding to a linear relationship for ln(N) in Fig. 1) is not expected, because selection of the size classes is arbitrary. Nevertheless, the observed distribution is remarkably close to an exponential relationship. The pattern breaks down only in the largest bins (≥64 mm), each with only a dozen or fewer clasts in the entire CRP-1 core.

A variety of glacial transport processes affects the size distribution of lonestones (*e.g.*, Kirkbride, 1995). For example, high-level portions of glaciers can have substantially higher lonestone volumes, relative to finer debris, than does the zone of basal traction, due to crushing in the basal zone (Boulton, 1978). Consequently, the shape of the exponential size/frequency trend, or the slope of a linear fit of ln(N) *versus* size class, may contain

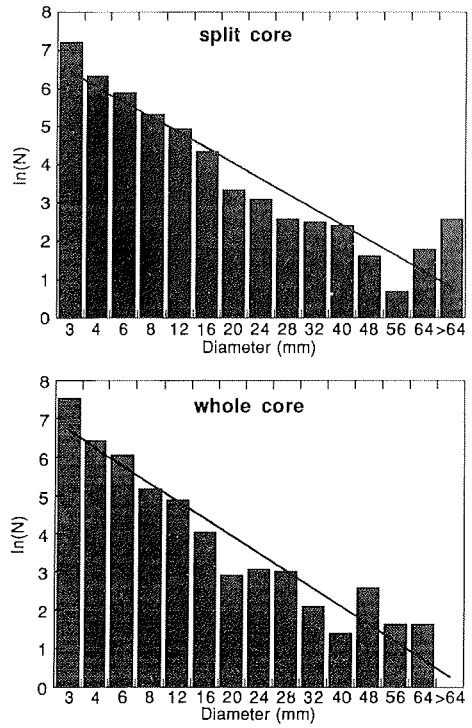

Fig. 1 - Size distribution of CRP-1 lonestones, based on image analysis of split-core (*a*) and whole-core (*b*) (outer core surface) images. The exponential size/frequency distribution for each dataset leads to a similar, approximately linear decrease in logarithm of number of lonestones with increasing size.

information concerning these processes. To investigate the possibility of systematic changes in size distribution, we plotted the size distribution separately for four lonestone-rich intervals: 30-43, 103-110, 119-135, and 135-141 mbsf (Fig. 2). No significant changes in the size distribution are observed. Analysis of whole-core data (L_{UUw}) yielded similar size distributions and confirmed the lack of systematic differences between 103-110 and 119-135 mbsf diamictites (Fig. 2). Because the number of points within these intervals is much smaller than for figure 1, substantial dispersion from the linear fit is evident at sizes as small as 20 mm, where sample size within a bin can be <10. Higher resolution, 1 m interval analyses of

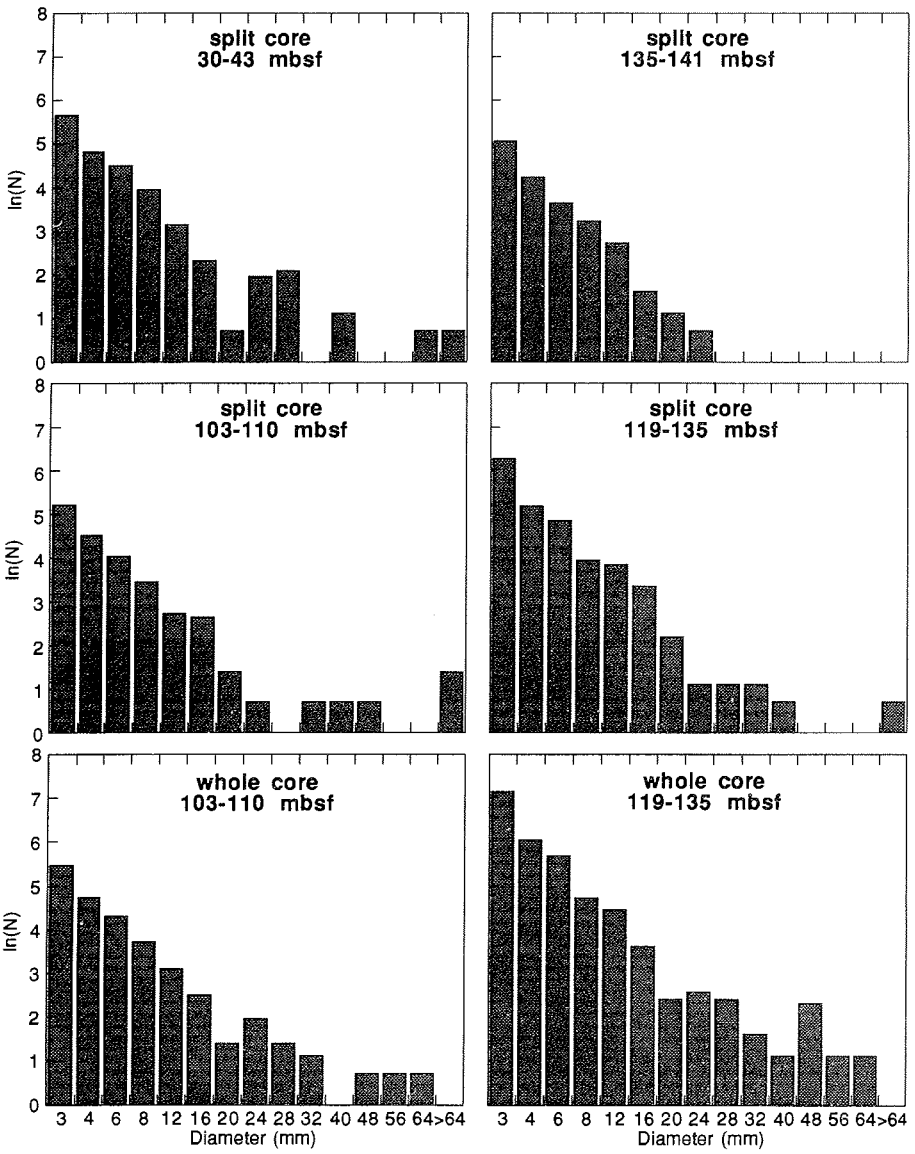

Fig. 2 - Size distribution of CRP-1 lonestones for individual lonestone-rich intervals. Note the similarity of split-core and whole-core results, and the similarity among intervals, for 3-16 mm particles.

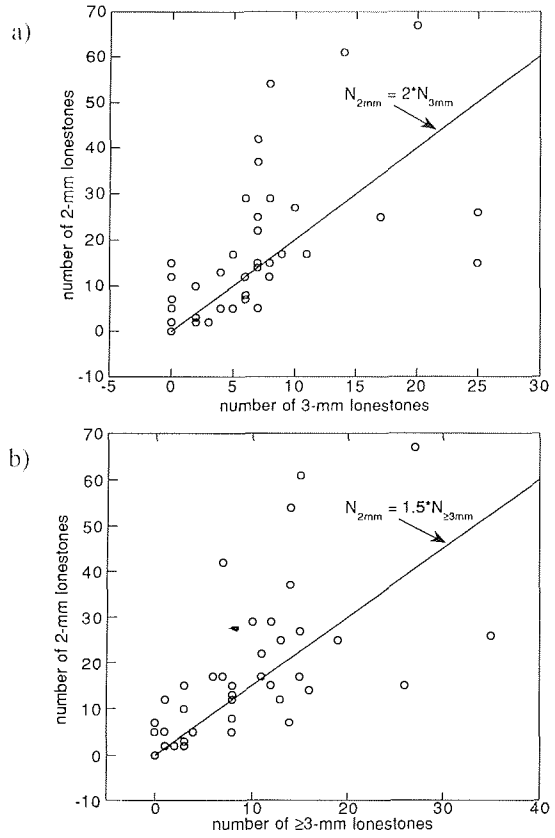

Fig. 3 - Comparison of number of 2-mm lonestones per 10 cm interval to both number of 3-mm lonestones (*a*) and number of 3-mm or larger lonestones (*b*). On average, 2-mm lonestones are roughly twice as abundant as 3-mm ones, and more abundant than all larger lonestones combined.

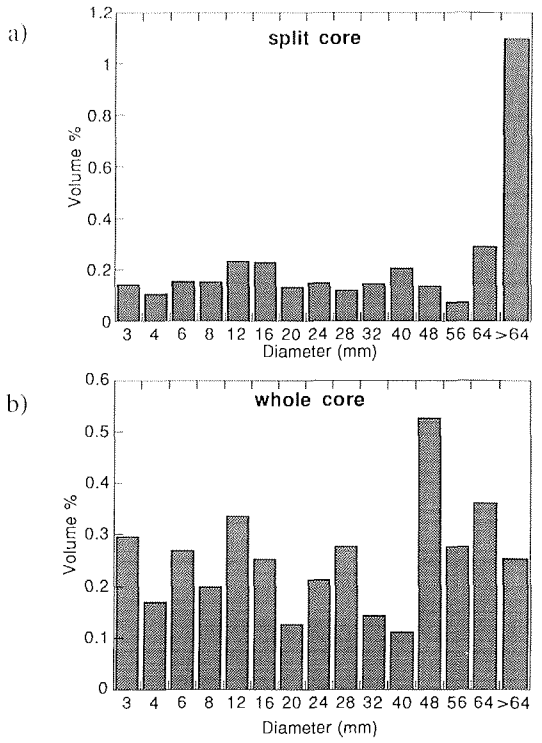

Fig. 4 - Size distribution of total lonestone volume, based on image analysis of split-core (*a*) and whole-core (*b*) images. Except for the largest lonestones, most size classes are present in about the same volume percentage, within a factor of two, despite the exponential drop in number of lonestones with increasing size (Fig. 1).

variations in size distribution had too few samples to detect any real changes that may be present.

Sizes >16 mm have rare enough lonestones that their counts are nonrepresentative when based on short intervals of split core. For example, 20-56 mm lonestones fit an exponential trend for the entire CRP-1 core (Fig. 1), but not for shorter intervals (Fig. 2). This problem does not affect total counts significantly, but it does affect local estimates of size distribution. For size classes of 16 mm or less, percentage fluctuations appear to be similar from interval to interval. This pattern is most readily tested for the smallest size class, 3 mm, which (as discussed above) exhibits no apparent systematic variations in percentage as a function of depth. This similarity in percentage fluctuations has an important corollary for lonestone abundance interpretations: the accuracy of the total lonestone count for any zone is dominated by fluctuations in the smallest class, in this case 3 mm, the class containing about half of all lonestones.

The analysis of lonestone size distribution can be extended to smaller sizes than the 3-mm minimum used in L_{UUs} analyses, based on the L_{FSU} counts of 2 mm, 3 mm, and >3 mm lonestones for selected 10-cm intervals. In figure 3a 2-mm lonestones are plotted *versus* 3-mm N_{FSU} for the 39 analysed 10-cm intervals, and figure 3b does the same for 2 mm *versus* ≥3 mm. Dispersion is high, in part because of the difficulty of accurately counting >20 tiny 2-mm particles within a very short interval. Nevertheless, a general pattern is evident: most intervals have approximately twice as many 2 mm lonestones as 3 mm ones, and approximately 1-1.5 times as many 2 mm lonestones as all larger sizes combined. This pattern is compatible with that for the detailed size distribution analyses of figure 1, showing approximately a doubling of lonestone count for each step downward in size class.

These observations lead to an important generalisation concerning lonestone abundance-counting: one can arbitrarily select any minimum-size cutoff, as long as one avoids dispersion associated with insufficient samples. However, care is needed to avoid any drift in this cutoff point, because about half of points are within the smallest size category selected. A lonestone-size overlay template is extremely useful in avoiding such drift.

LONESTONE VOLUME

Lonestone volume percentage (V_{UUs} or V_{UUw}) for each 10-cm interval can be estimated from its L_{UUs} or L_{UUw} lonestone-size-distribution counts: $V(\%) = 100*\Sigma(N_i\pi r_i^2)/A$, where N_i is the number of lonestones of radius r_i, and A is the area of split-core or whole-core surface. Volume percentage (V_{CRC}) was also visually estimated along with the N_{CRC} determinations during initial core descriptions, and plotted in the CRP Initial Reports (Cape Roberts Science Team, 1998).

The contribution made by different size fractions to overall lonestone volume is shown in figure 4. Within a factor of approximately two, most size classes contribute

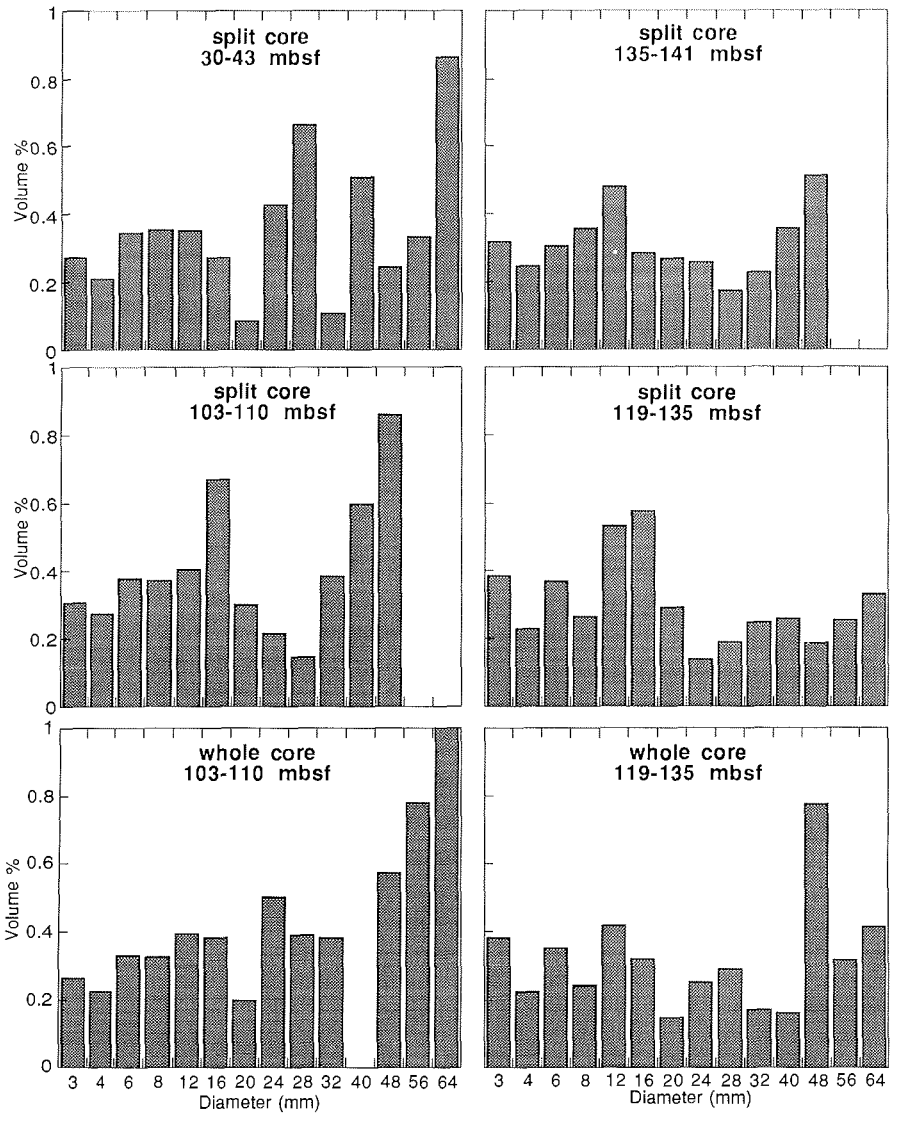

Fig. 5 - Size distribution of lonestone volume for individual lonestone-rich intervals. Note that particles larger than about 16 mm exhibit high variability, both between intervals and between split-core and whole-core results for the same interval; this heterogeneity is attributed to the rare and therefore nonrepresentative sampling of larger lonestones. Heterogeneity for lonestones >64 mm was too great to even be shown on this plot. Note also the consistency of split-core and whole-core results for 3-12 mm particles for the depth intervals 103-110 and 119-135 mbsf.

the same volume to the total. Boulton (1978) reached a similar conclusion for 2-16 mm lonestones within the zone of basal traction of three active glaciers. In the largest classes (≥48 mm), lonestone counts per class are too low for representative sampling, leading to large fluctuations. L_{UUs} and L_{UUw} did not include 2-mm lonestones. The L_{FSU} data show difference by a factor of two between 2- and 3-mm lonestone abundances (Fig. 3a), indicating similar total volumes for 2-mm and 3-mm lonestones.

The exponential decrease in lonestone number is compensated by an increase in volume per clast. The impact of random fluctuations and sampling error on the two distributions is quite different, however. Fluctuations in number of the largest lonestones have negligible influence on total lonestone abundance but, because of their large volumes, they cause major fluctuations in total lonestone volume (Fig. 4). This effect can be seen more clearly by examining volume distributions for shorter intervals. As shown by figure 5, the contributions to total volume for sizes of ≤16 mm are relatively stable from interval to interval. In contrast, the contributions for larger sizes are extremely variable, because too few lonestones are observed for a representative sample.

Despite the small number of lonestones >16 mm in size - seldom more than 1-3 per metre - the volume of such lonestones can dominate the entire pattern of lonestone-volume changes as a function of depth. Figure 6 plots lonestone volume *versus* depth, both for all lonestones and for lonestones ≤16 mm in size. Also shown is the number of these largest lonestones per 1-m interval. Clearly, inclusion of these largest lonestones causes a major increase in fluctuations in lonestone volume. Very high variability is similarly shown by the semiquantitative CRC estimates of lonestone volume (Fig. 6). Total lonestone volume, whether measured by image analysis or visually estimated, is dominated by these rare lonestones.

Total lonestone volume, calculated from the size distribution of all lonestones (dotted line in Fig. 6a), accurately describes lonestone variations within the CRP-1 cores. However, it is not the best estimate of volume variations *in situ*. The volume of sediment contained in the CRP-1 core is too small to provide an accurate indication of either the number or volume of *in situ* lonestones >16 mm within short intervals. This possible bias can be minimized by confining the analysis to lonestones ≤16 mm in diameter. The ≤16 mm lonestones

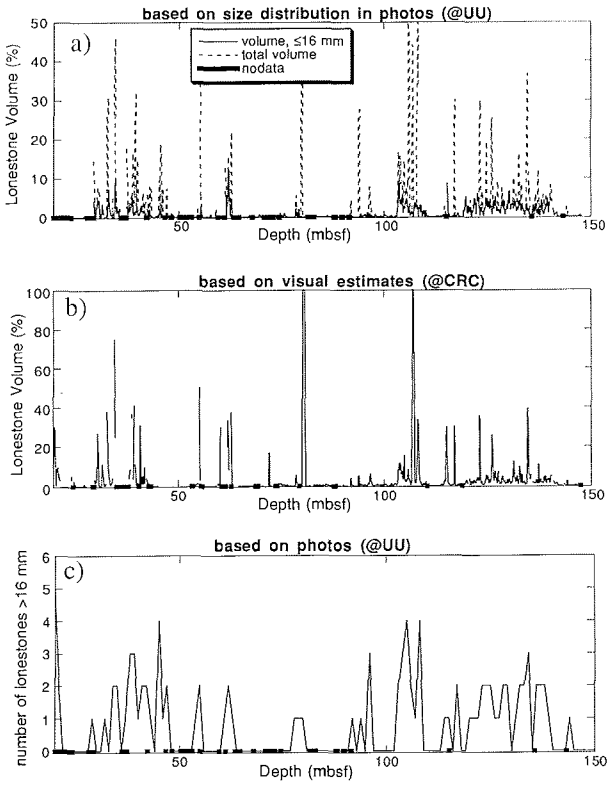

Fig. 6 - Variations in lonestone volume *vs* depth, based on quantitative image analysis (*a*) and visual estimation (*b*). Spikiness of the two total lonestone plots is attributable to the very rare occurrence of large (>16 mm) lonestones (*c*). In contrast, variations in volume of the smaller lonestones (top plot, solid line) are more regular. Heavy solid line segments at the base of each plot indicate data gaps.

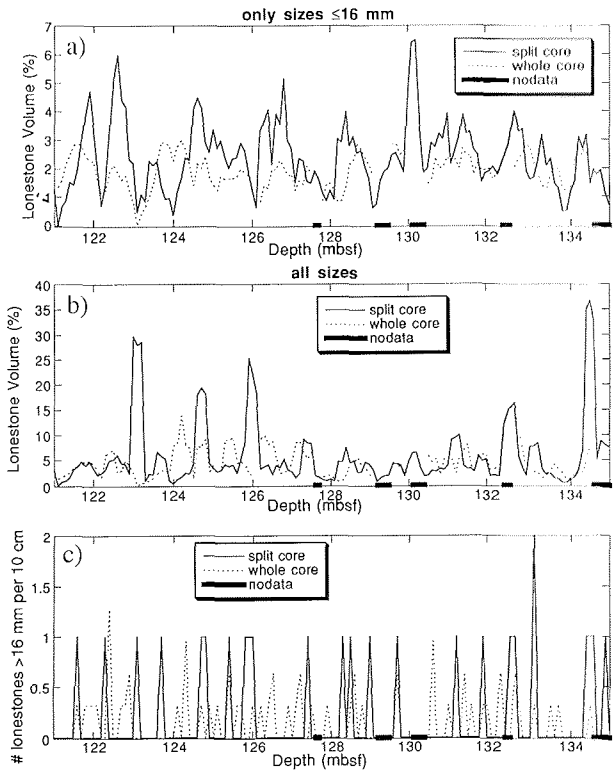

Fig. 7 - Comparison of split-core and whole-core results of image analysis for the same depth interval. Number of large (>16 mm) lonestones per 10 cm interval is so low that split and whole cores cannot give consistent, representative counts (*c*). These rare, large lonestones dominate portions of the log of total lonestone volume (*b*), leading to occasional large inconsistencies between split-core and whole-core estimates. Confining the lonestone volume calculation to sizes ≤16 mm removes this instability and gives generally consistent results for the two independent samples (*a*). Heavy solid line segments at the base of each plot indicate data gaps.

are present in sufficient quantity for the CRP-1 core to obtain a representative sample of their variations. The ≤16 mm lonestones represent only about half of total lonestone volume (Figs. 4 & 5), but they provide a more robust measure of true variations in lonestone volume *versus* depth or age than can be obtained by including all sizes in the calculation.

Figure 7 tests and confirms this conclusion that excluding >16 mm lonestones provides a more representative sample of lonestone volumes. This figure compares results from the core outer surface to those from split core, thereby sampling lonestone populations that are independent (except for the largest lonestones). The comparison is confined to the interval 121-135 mbsf, the most continuous interval of available whole-core images. The number of lonestones >16 mm per 10-cm interval (or, for whole-core data, N/π because the sampled area is π times larger than for split core) shows very little correlation for these two independent samples of identical stratigraphic section. Because of its sensitivity to these rare lonestones, total lonestone volume for the two datasets is sometimes poorly correlated. In contrast, lonestone volume for sizes ≤16 mm exhibits a much better correlation between the two datasets. Even for these smaller sizes, discrepancies are evident (*e.g.*, 124 mbsf), indicating that the available core area is sufficient to give reasonably, but not perfectly, representative samples.

LONESTONE ABUNDANCE

Figure 8 summarises CRP-1 lonestone abundance variations as a function of depth, based on both visual counts at Cape Roberts Camp (N_{CRC}) and image analysis of split-core images at University of Utah (N_{UUs}). Also shown, as a heavy bar along the base of each plot, are intervals for which no core was obtained or accurate picks could not be determined. For the interval between the 43.15 mbsf (the top of the Miocene section) and about 93 mbsf, lonestone abundance was generally low but often could not be quantified because of brecciation or other factors described earlier.

The broad patterns of lonestone abundance variations estimated by the two methods are quite consistent, as are most of the smaller-scale fluctuations as well. This agreement is not surprising, as both counts considered the same split-core face. In view of the different limitations of the two counting methods, the agreement is encouraging.

INTERPRETATION

Our two best estimates of CRP-1 lonestone abundance are lonestone volume for ≤16-mm clasts ($V_{\leq 16}$) and total

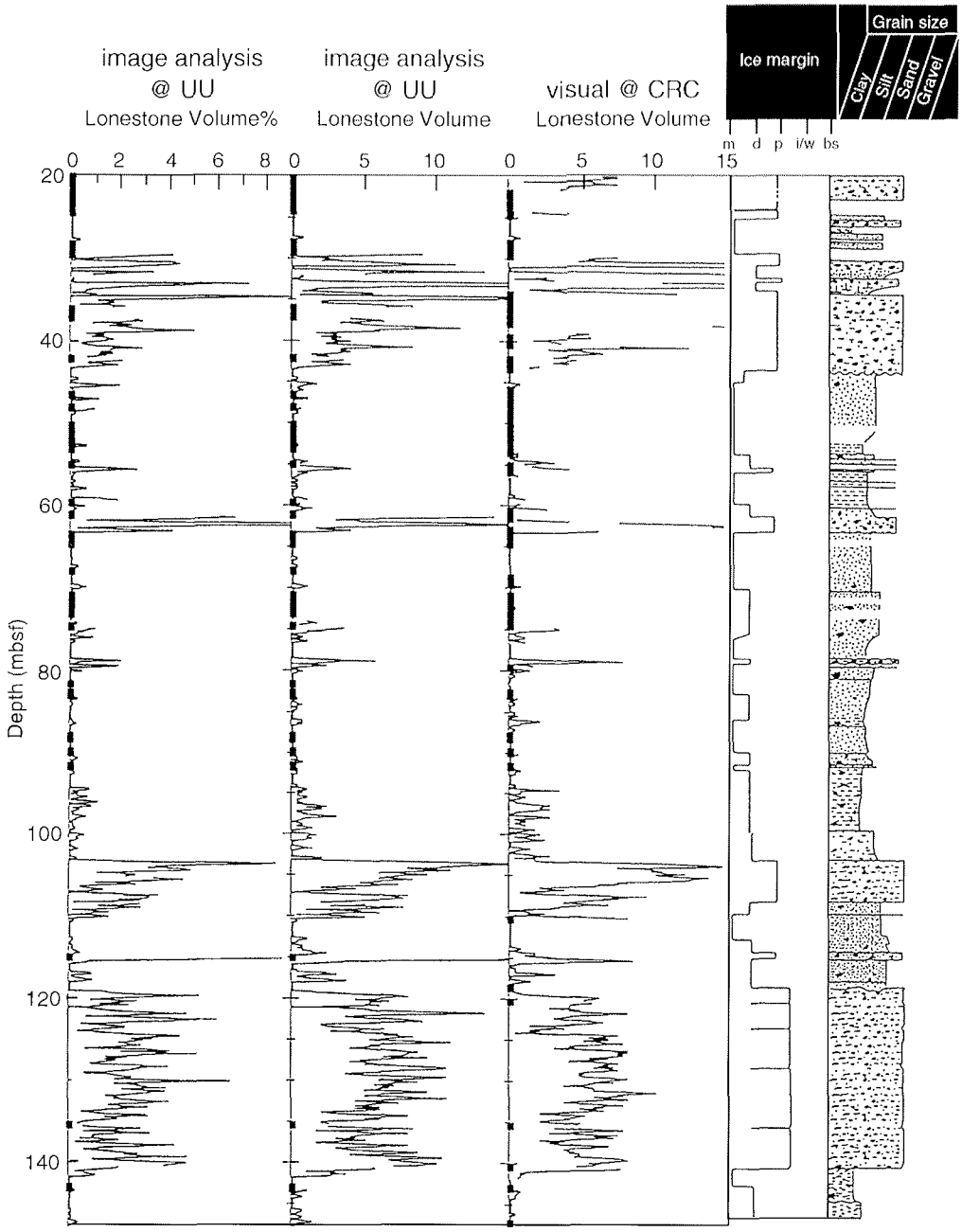

Fig. 8 - Variations in lonestone abundance *vs* depth, based on visual estimation and image analysis. Agreement is generally good. Heavy solid line segments along the margin of each plot indicate data gaps. Variations in visual lonestone abundance are based on Cape Roberts Camp analysis. Variations in lonestone abundance and volume from the University of Utah study are based on split-core image analysis. Major variations are well correlated with initial estimates of proximity of the ice margin to the site: marine (m), distal glaciomarine (d), proximal glaciomarine (p), ice contact/waterlain till (i/w), and basal till (b) (Cape Roberts Science Team, 1998). Lonestone variations also generally correspond with core lithostratigraphy (Cape Roberts Science Team, 1998).

number of lonestones (N_{UUs}), both determined by image analysis of split-core images. Although the two measures are obtained from the same core face, they emphasize different features. Lonestone volume weights the different size fractions relatively equally, whereas total lonestone number weights the smallest lonestones most heavily. Both $V_{\leq 16}$ and N_{UUs} are robustly determined, based on sufficient data to be applicable for high-resolution (*e.g.*, 10-cm) studies. Features that are evident with both measures are likely to be more reliably determined than those based on only one.

CRP-1 lonestone abundance has been used as an indicator of proximity of the ice margin to the drill site (Cape Roberts Science Team, 1998). This initial analysis was based mainly on the N_{CRC} counts, because clast percentage (V_{CRC}) was recognised as being locally dominated by rare, large clasts. Our two best indicators of lonestone abundance confirm and refine the patterns seen in the N_{CRC} results (Fig. 8); they do not provide independent evidence of variations in ice-margin proximity. Factors that complicate such an association between lonestone abundance and ice-margin proximity include redeposition

of lonestones by debris flows, redeposition of muds and sands by turbidity currents, variable input of meltwater, and the possibility that maximum lonestone supply occurs during glacial retreat rather than at maximum glacial advance.

Large-scale changes in lonestone abundance are linked to the CRP-1 sequence stratigraphy (Cape Roberts Science Team, 1998; Fielding et al., this volume). The basal portion of most CRP-1 sequences is diamict, and lonestone abundance is generally higher in diamicts than in other CRP-1 sediments. The dominant sequence stratigraphic pattern at the site is interpreted to be transgressive – consisting of shallow-water diamicts followed by deeper-water sands and muds (Cape Roberts Science Team, 1998; Fielding et al., this volume) – although the relationship between lithology and water depth is recognised to be more complex in detail (*e.g.*, Fielding et al., this volume; Howe et al., this volume; Powell et al., this volume).

Transgressions have not, however, generated patterns of gradual decrease in lonestone abundance within each sequence. Instead, sequences are evident in figure 8 as generally bimodal alternations between lonestone-rich diamict and lonestone-poor sands and muds, and neither exhibits a systematic internal pattern of gradual lonestone decrease. Discontinuous sedimentation of at least one component has probably obscured most of the original gradual changes in lonestone deposition. Estimated net accumulation rates at CRP-1 (Cape Roberts Science Team, 1998) are several orders of magnitude lower than observed modern sedimentation rates of similar facies (Powell et al., this volume), suggesting that only brief snapshots of overall transgressive sedimentation survive.

Two large-scale, saw-toothed lonestone abundance patterns are identified. Unit 6.1 (103.1-108.8 mbsf based on cores, or 103-111 mbsf based on lonestones or physical properties (Niessen et al., this volume)), contains two 4-m thick cycles of gradually increasing lonestone abundance followed by sudden drops, at 111-107 and 107-103 mbsf (Fig. 8). Another cycle of gradual increase may be present in the basal Quaternary section (Fig. 8). Webb & Strong (this volume) document faunal evidence that Quaternary glacial fluctuations at CRP-1 are recorded as gradual advances and sudden retreats.

If local glacial maxima are accompanied by both eustatic sea level minima and lonestone abundance peaks, then these 2-3 gradual lonestone increases appear to be more compatible with regressions during glacial advances than with transgressions. In contrast, the CRP-1 sequences are interpreted as being almost entirely transgressive, with sedimentary evidence of regressive progradational periods removed by erosion (Cape Roberts Science Team, 1998). Possibly, these three gradual lonestone increases are exceptions to that generalisation. If, alternatively, these units are transgressive, then the gradual lonestone increases may result from meltwater increase during glacial retreat.

Implicit in the association between lonestone abundance and ice-margin proximity is the assumption that lonestone supply from glacial processes dilutes a relatively steady supply of fine-grained sediments. Grain-size analyses of CRP-1 diamicts appear to be compatible with this assumption: gravel and coarse-sand lonestone fluctuations are superimposed on an otherwise log-normal distribution about a mean grain size near the sand/silt boundary (De Santis & Barrett, this volume; Woolfe et al., this volume). Even if this assumption is valid for large-scale fluctuations such as those that dominate figure 8, it may not be valid for high-frequency variations because the supply of fine grained sediments may vary with meltwater supply. A strong 0.5-0.7 m periodicity evident below 120 mbsf (Fig. 8) may be caused either by fluctuations of the ice margin or by individual debris flows. If fluctuations of the ice margin are responsible for this lonestone periodicity, then a saw-toothed lonestone depositional pattern may be predicted. For example, binge-purge ice stream behavior might be expected to create a sudden increase in lonestones during a rapid local advance, followed by a gradual decrease as local glacial supply wanes. However, the lonestone abundance fluctuations are generally symmetrical, not saw-toothed. Comparison of trough-to-peak rise lengths to peak-to-trough decay lengths for this interval shows no evidence of a statistically significant difference between the two. This conclusion is not changed by using 3-point or 5-point smoothing to bypass the highest frequency fluctuations. Any depositional mechanism proposed to account for the 0.5-0.7 m lonestone periodicity should also account for the symmetrical character of these fluctuations.

ACKNOWLEDGEMENTS

We thank Tim Paulsen for his work on digital imaging of the CRP-1 cores and his advice to us concerning methods for handling these data. We also thank Ken Woolfe and Gene Domack for providing constructive reviews of this paper. This research was supported by the National Science Foundation (OPP-9418429).

REFERENCES

Bennett M.R., Hambrey M.J. & Huddart D., 1997. Modification of clast shape in high-arctic glacial environments. *J. Sedim. Res.*, **67**, 550-559.

Boulton G.S., 1978. Boulder shapes and grain-size distributions of debris as indicators of transport paths through a glacier and till genesis. *Sedimentology*, **25**, 773-799.

Cape Roberts Science Team, 1998. Initial Report on CRP-1, Cape Roberts Project, Antarctica. *Terra Antartica*, **5**(1), 187 p.

Domack E.W., Anderson J.B. & Kurtz D.D., 1980. Clast shape as an indicator of transport and depositional mechanisms in glacial marine sediments: George V Continental Shelf, Antarctica. *J. Sed. Pet.*, **50**, 813-820.

Hambrey M.J., 1989. Grain fabric. In: Barrett P.J. (ed.), *Antarctic Cenozoic History from the CIROS-1 Drillhole, McMurdo Sound, Antarctica, DSIR Bulletin*, **245**, 59-62.

Kirkbride M.P., 1995. Processes of transportation. In: Menzies J. (ed.), *Modern Glacial Environments: Processes, Dynamics and Sediments*, Butterworth-Heinemann, Oxford UK, 261-292.

Krumbein W.C., 1941. Measurement and geological significance of shape and roundness of sedimentary particles. *J. Sed. Pet.*, **11**, 64-72.

Pettijohn F.J., Potter P.E. & Siever R., 1987. *Sand and Sandstone*. Springer-Verlag, New York, 553 p.

Sharp M., 1982. Modification of clasts in lodgement tills by glacial erosion. *Journal of Glaciology*, **28**, 475-481.